



## Exploiting *in-situ* solid-state NMR spectroscopy to probe the early stages of hydration of calcium aluminate cement

Colan E. Hughes<sup>a</sup>, Brant Walkley<sup>b</sup>, Laura J. Gardner<sup>b</sup>, Samuel A. Walling<sup>b</sup>, Susan A. Bernal<sup>b,c</sup>, Dinu Iuga<sup>d</sup>, John L. Provis<sup>b,\*\*</sup>, Kenneth D.M. Harris<sup>a,\*</sup>

<sup>a</sup> School of Chemistry, Cardiff University, Park Place, Cardiff, Wales, CF10 3AT, UK

<sup>b</sup> Department of Materials Science and Engineering, University of Sheffield, Sir Robert Hadfield Building, Mappin Street, Sheffield, S1 3JD, UK

<sup>c</sup> School of Civil Engineering, University of Leeds, Leeds, LS2 9JT, UK

<sup>d</sup> Department of Physics, University of Warwick, Coventry, CV4 7AL, UK

### ARTICLE INFO

#### Keywords:

*In-situ* solid-state NMR

<sup>27</sup>Al NMR

Calcium aluminate

CLASSIC NMR

Cement formation

### ABSTRACT

We report a high-field *in-situ* solid-state NMR study of the hydration of CaAl<sub>2</sub>O<sub>4</sub> (the most important hydraulic phase in calcium aluminate cement), based on time-resolved measurements of solid-state <sup>27</sup>Al NMR spectra during the early stages of the reaction. A variant of the CLASSIC NMR methodology, involving alternate recording of direct-excitation and MQMAS <sup>27</sup>Al NMR spectra, was used to monitor the <sup>27</sup>Al species present in both the solid and liquid phases as a function of time. Our results provide quantitative information on the changes in the relative amounts of <sup>27</sup>Al sites with tetrahedral coordination (the anhydrous reactant phase) and octahedral coordination (the hydrated product phases) as a function of time, and reveal significantly different kinetic and mechanistic behaviour of the hydration reaction at the different temperatures (20 °C and 60 °C) studied.

### 1. Introduction

The application of solid-state NMR spectroscopy to understand fundamental aspects of cement science has a long history [1–3]. Although cements often have complex compositions, solid-state NMR provides key information about the structures of some of the common components, particularly from solid-state <sup>27</sup>Al and <sup>29</sup>Si NMR measurements. However, while other experimental techniques (including soft X-ray imaging [4] and synchrotron X-ray powder diffraction [5]) have been applied for *in-situ* studies of hydration processes, previous NMR investigations have been limited to *ex-situ* studies, involving the examination of samples extracted at different stages during the hydration process and then dehydrated to halt the reaction before measurement of the solid-state NMR data [1,2,6,7]. In part, the focus on *ex-situ* studies to date has been dictated by technical challenges associated with sealing liquid-containing samples in standard solid-state NMR rotors and then subjecting these samples to magic-angle spinning (MAS) at frequencies of several kHz without leakage of the liquid into the NMR magnet. However, there has been significant progress in recent years in the development of sealing systems for carrying out MAS on liquid-containing samples, which

has facilitated the development of techniques for *in-situ* solid-state NMR studies of crystallization processes from solution [8–15]. In this paper, we report the first application of such *in-situ* NMR techniques to study the hydration of a hydraulic cement, namely calcium aluminate cement, which has a sufficiently high aluminium content to allow <sup>27</sup>Al NMR spectra to be recorded with comparatively short data collection times. We note, however, that earlier NMR studies [16–18] examined hydration of silicate materials under similar experimental conditions.

As the <sup>27</sup>Al nucleus is quadrupolar (spin  $I = 5/2$ ), direct-excitation <sup>27</sup>Al NMR spectra (recorded using a single <sup>27</sup>Al pulse) are typically characterized by broad lines even when the sample is subjected to MAS. While the second-order broadening of the central transition may, in principle, yield information on the electronic configuration around the <sup>27</sup>Al nucleus, the line-broadening is often problematic in the study of complex materials or mixtures of solid phases as it can lead to substantial overlap of signals from different <sup>27</sup>Al sites. As the line broadening is inversely proportional to the applied magnetic field, it can be advantageous to record <sup>27</sup>Al NMR data at high magnetic field. For this reason, the <sup>27</sup>Al NMR experiments reported here have been carried out at high magnetic field (20 T; <sup>27</sup>Al Larmor frequency, 221.54 MHz) at the U.K.

\* Corresponding author.

\*\* Corresponding author.

E-mail addresses: [j.provis@sheffield.ac.uk](mailto:j.provis@sheffield.ac.uk) (J.L. Provis), [HarrisKDM@cardiff.ac.uk](mailto:HarrisKDM@cardiff.ac.uk) (K.D.M. Harris).

<https://doi.org/10.1016/j.ssnmr.2019.01.003>

Received 18 October 2018; Received in revised form 11 January 2019; Accepted 11 January 2019

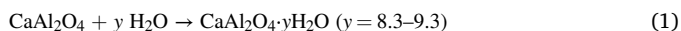
Available online 14 January 2019

0926-2040/© 2019 The Authors. Published by Elsevier Inc. This is an open access article under the CC BY license (<http://creativecommons.org/licenses/by/4.0/>).

National High-Field Solid-State NMR Facility. It is also advantageous to utilize one of the techniques that allow isotropic NMR spectra to be recorded for nuclei of half-integer spin, such as  $^{27}\text{Al}$ , and here we use the MQMAS technique [19] in our *in-situ*  $^{27}\text{Al}$  NMR studies.

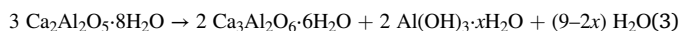
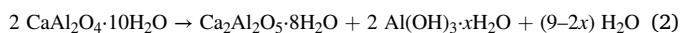
To assess the capability of *in-situ* solid-state  $^{27}\text{Al}$  NMR to study cement hydration, we focus on calcium aluminate cement (CAC). Calcium aluminate cements consist primarily of calcium aluminate ( $\text{CaAl}_2\text{O}_4$ ) with smaller quantities of mayenite ( $\text{Ca}_{12}\text{Al}_{14}\text{O}_{33}$ ), calcium dialuminate ( $\text{CaAl}_4\text{O}_7$ ) and/or aluminium oxide ( $\text{Al}_2\text{O}_3$ ), together with some impurities containing iron and/or silicon. The CAC system was selected for our *in-situ* solid-state NMR study for three reasons: (i) it is industrially important as a refractory and/or high early strength cement, and as a constituent for specialty mortars (for example, for self-levelling applications and niche applications such as storage of radioactive waste [20–22]), (ii) it has near neutral pH, which minimizes potential hazards for the seals on the NMR rotors used in our *in-situ* NMR studies, and (iii) it represents a suitable model system due to its simplicity in comparison to other common cements such as Portland cement. Nevertheless, to understand the structural changes that occur as the cement hardens from a freshly mixed slurry to a monolithic solid, time-resolved *in-situ* analysis is essential.

Different reaction pathways are anticipated in the initial stages of hydration of CAC in different temperature regimes. Below *ca.* 15 °C, reaction of  $\text{CaAl}_2\text{O}_4$  with water has been observed [23] to produce predominantly the so-called “calcium aluminate decahydrate” ( $\text{CaAl}_2\text{O}_4 \cdot 10\text{H}_2\text{O}$ ). However, we note that recent work [24] suggests that the stoichiometry of this material actually varies between about 8.3 and 9.3 water molecules per formula unit, as shown in Equation (1):

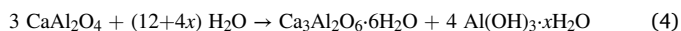


Nevertheless, for consistency with previous literature, we refer to this material subsequently as  $\text{CaAl}_2\text{O}_4 \cdot 10\text{H}_2\text{O}$ .

At temperatures in the approximate range [25] 15 °C – 30 °C, it has been suggested [22,23] that the main initial product is  $\text{Ca}_2\text{Al}_2\text{O}_5 \cdot 8\text{H}_2\text{O}$ , possibly with the concomitant formation of  $\text{CaAl}_2\text{O}_4 \cdot 10\text{H}_2\text{O}$  (particularly when the temperature is near ambient temperature). Both  $\text{CaAl}_2\text{O}_4 \cdot 10\text{H}_2\text{O}$  and  $\text{Ca}_2\text{Al}_2\text{O}_5 \cdot 8\text{H}_2\text{O}$  are metastable and ultimately undergo dehydration and structural rearrangement to form two stable phases:  $\text{Ca}_3\text{Al}_2\text{O}_6 \cdot 6\text{H}_2\text{O}$  (tricalcium aluminate hexahydrate, a hydrogarnet type phase) and  $\text{Al}(\text{OH})_3 \cdot x\text{H}_2\text{O}$  with small values of  $x$  less than *ca.* 0.2 (a structurally disordered, hydrated form of aluminium hydroxide). Equations (2) and (3) describe this process in a stepwise form:



At sufficiently high temperature [22], hydration of  $\text{CaAl}_2\text{O}_4$  may lead directly to the formation of  $\text{Ca}_3\text{Al}_2\text{O}_6 \cdot 6\text{H}_2\text{O}$  and  $\text{Al}(\text{OH})_3 \cdot x\text{H}_2\text{O}$ , according to Equation (4):



In anhydrous  $\text{CaAl}_2\text{O}_4$ , aluminium is present only in sites with approximately tetrahedral coordination, whereas in the hydrate phases, aluminium is present in sites with approximately octahedral coordination (the crystal structures [24,26] of  $\text{CaAl}_2\text{O}_4 \cdot 10\text{H}_2\text{O}$  and  $\text{Ca}_3\text{Al}_2\text{O}_6 \cdot 6\text{H}_2\text{O}$  both have a single octahedrally-coordinated  $^{27}\text{Al}$  site). Thus, the isotropic  $^{27}\text{Al}$  NMR chemical shifts for the hydrate phases should be clearly distinct from those for anhydrous  $\text{CaAl}_2\text{O}_4$ . However, resolving the  $^{27}\text{Al}$  NMR signals for the octahedral sites in the different hydrate phases is more challenging. Indeed, previous *ex-situ*  $^{27}\text{Al}$  NMR studies [1,2], in which samples were extracted at different stages during the hydration process and then dehydrated (by treatment with acetone and ether) before recording  $^{27}\text{Al}$  NMR spectra, demonstrated the change in coordination of the  $^{27}\text{Al}$  sites from tetrahedral to octahedral, but were unable to identify the specific phases produced.

In the recently reported CLASSIC NMR methodology [27], different

types of NMR spectrum are recorded alternately during *in-situ* studies of crystallization from solution, allowing the time-evolution of both the liquid and solid phases to be monitored effectively simultaneously in the same experiment. In the present work, we have implemented a similar strategy involving alternate recording of direct-excitation and MQMAS  $^{27}\text{Al}$  NMR spectra during the *in-situ* time-resolved study of hydration of CAC. In the direct-excitation spectra, we expect to observe all  $^{27}\text{Al}$  sites in the system, including those in solid and liquid phases. In the MQMAS spectra, on the other hand, we expect to observe signals only from  $^{27}\text{Al}$  sites in solid phases for which the multiple-quantum excitation and reconversion pulses are relatively efficient.

## 2. Experimental Methods

$^{27}\text{Al}$  NMR spectra were recorded at 20.0 T on a Bruker AVANCE III spectrometer at the U. K. High-Field (850 MHz) Solid-State NMR Facility ( $^{27}\text{Al}$  Larmor frequency, 221.5 MHz) with a 4 mm HXY probe (MAS frequency, 10 kHz) and a zirconia rotor with a “high-resolution” insert for liquid-containing samples. The “high-resolution” inserts (also known as “HR-MAS”) were purchased from Bruker and used without modification; they are made of Kel-F and consist of a tube into which the sample is placed, followed by sealing with a plug and screw.

Chemical shifts were referenced *via* a secondary standard of YAG (yttrium aluminium garnet) with the hexa-coordinated site referenced to 0.7 ppm, which corresponds to the standard reference of  $^{27}\text{Al}$  in 1 M aqueous  $\text{Al}(\text{NO}_3)_3$  at 0 ppm. A commercial sample of CAC (Secar 71, Kerneos, France) was used in this work; this material comprises predominantly (*ca.* 55%) calcium aluminate ( $\text{CaAl}_2\text{O}_4$ ) together with calcium dialuminate ( $\text{CaAl}_4\text{O}_7$ ) and aluminium oxide ( $\text{Al}_2\text{O}_3$ ). For our *in-situ*  $^{27}\text{Al}$  NMR studies, the sample of CAC was mixed with water at a water/Secar 71 mass ratio of 0.35 (which corresponds to a water/ $\text{CaAl}_2\text{O}_4$  mass ratio of 0.64). This low ratio was selected as it gives a thick paste, which should minimize the likelihood of phase segregation occurring due to the centrifugation effect of applying MAS to the NMR rotor. The resulting paste was injected into the “high-resolution” insert which was sealed and fitted into the rotor. The rotor was then inserted into the NMR spectrometer, which was already set to the required temperature (20 °C or 60 °C). Sample temperatures were set according to a calibration using lead nitrate [28] and verified in the temperature range of our experiments by measurements on methanol [29–31], taking into consideration the heating effect due to MAS. Data acquisition started within 10 min of the initial mixing of CAC and water.

To record the MQMAS  $^{27}\text{Al}$  NMR spectra, a  $z$ -filtered 3QMAS pulse sequence [32,33] was used with a double-frequency sweep on the 3Q to 1Q conversion pulse [34]. The resulting spectra were sheared using standard Bruker TOPSPIN software. Each direct-excitation spectrum was acquired in 1.1 min (64 scans; recycle delay, 1 s) and each MQMAS spectrum was acquired in 22.2 min (64  $t_1$  increments with 96 scans and 4 dummy scans per increment; recycle delay, 0.2 s). Thus, the overall time resolution of our *in-situ* NMR study was 23.3 min. Radio-frequency field strengths in the MQMAS experiment were 60 kHz for the excitation pulse, 9 kHz for the selective pulse and 30 kHz for the double-frequency sweep.  $^1\text{H}$  decoupling was not applied in any of our experiments.

Isothermal calorimetry experiments were carried out at base temperatures of (20.00 ± 0.02) °C and (60.00 ± 0.02) °C using a TAM Air calorimeter. The fresh cement paste was prepared by external hand-mixing for 3 min, weighed into an ampoule and immediately placed into the calorimeter to record heat flow for the first 300 h of the hydration reaction. All results are normalized by the total mass of the paste.

## 3. Results and discussion

### 3.1. Characterization of the CAC starting material

The direct-excitation  $^{27}\text{Al}$  NMR spectrum of the starting sample of CAC is shown in Fig. 1a. The intense group of peaks between 76 and

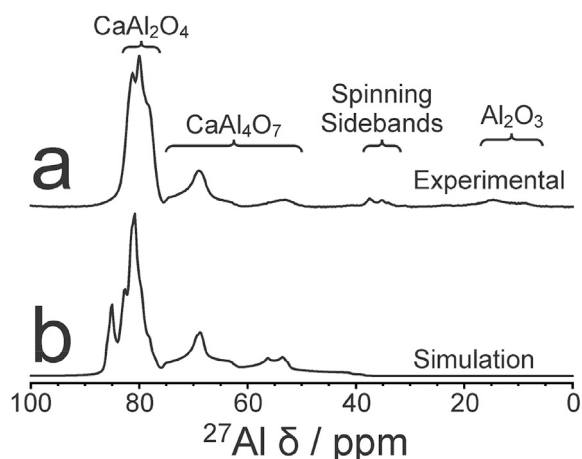


**Fig. 1.** (a) Experimental direct-excitation  $^{27}\text{Al}$  NMR spectrum recorded for the starting sample of CAC [42]. (b) Simulated  $^{27}\text{Al}$  NMR spectrum for a 1.5:1 ratio of  $\text{CaAl}_2\text{O}_4$  and  $\text{CaAl}_4\text{O}_7$ , calculated using the contour analysis method [43] with line broadening of 0.25 ppm.

84 ppm is due to  $\text{CaAl}_2\text{O}_4$ , which has six distinct  $^{27}\text{Al}$  environments. The peaks between 50 and 75 ppm are assigned [3] to the two distinct  $^{27}\text{Al}$  environments in  $\text{CaAl}_4\text{O}_7$  and the peaks between 5 and 20 ppm are assigned [35] to  $\text{Al}_2\text{O}_3$ , both of which were also present in the CAC sample (see Experimental Methods). Spinning sidebands due to  $\text{CaAl}_2\text{O}_4$  are also observed (between 33 and 39 ppm) in Fig. 1a.

Values of isotropic  $^{27}\text{Al}$  chemical shifts and  $^{27}\text{Al}$  quadrupolar coupling constants for  $\text{CaAl}_2\text{O}_4$  and  $\text{CaAl}_4\text{O}_7$  have been reported by Skibsted et al. [3] The simulated  $^{27}\text{Al}$  NMR spectrum (Fig. 1b) for a mixture of  $\text{CaAl}_2\text{O}_4$  and  $\text{CaAl}_4\text{O}_7$  in 1.5:1 molar ratio, calculated using these isotropic chemical shifts and quadrupolar coupling constants for the  $^{27}\text{Al}$  Larmor frequency (221.5 MHz) used in the present work, is in good qualitative agreement with our experimental data (Fig. 1a).

### 3.2. *In-situ* $^{27}\text{Al}$ NMR study of the hydration reaction at 20 °C

Our *in-situ*  $^{27}\text{Al}$  NMR experiment on the mixture of the anhydrous CAC sample and water at 20 °C was run for a total of 21 h. The direct-excitation  $^{27}\text{Al}$  NMR spectra recorded as a function of time during this experiment are shown in Fig. 2 (only every fifth recorded spectrum is displayed, representing a time interval of 116 min between the spectra shown). First, we note that the contributions due to  $\text{CaAl}_4\text{O}_7$  and  $\text{Al}_2\text{O}_3$  remain unchanged as a function of time as these phases do not participate in the hydration reaction. Thus, the changes in the  $^{27}\text{Al}$  NMR spectra as a function of time result *only* from the hydration of  $\text{CaAl}_2\text{O}_4$ .

From the start of the hydration process, a new feature appears in the  $^{27}\text{Al}$  NMR spectrum between ca. 5 ppm and 16 ppm, superimposed on the peak due to  $\text{Al}_2\text{O}_3$ . Clearer insights into the emergence and evolution of the new feature are gained by subtracting the second spectrum recorded [36] (which, in the spectral region from 5 ppm to 16 ppm, contains only the peak due to  $\text{Al}_2\text{O}_3$ ) from all subsequent spectra, revealing the growth of the new peak centred at ca. 11 ppm (Fig. 3). Integration of the region between 5 and 16 ppm as a function of time in the data shown in Fig. 3 yields kinetic information on the growth of the new peak and a plot of peak intensity (scaled relative to the peaks for  $\text{CaAl}_2\text{O}_4$  in the second spectrum) is shown in Fig. 4. It is clear that initial growth of the new peak occurs over the first 5 h of the experiment but the growth is then much slower between 5 h and 16 h. However, after 16 h, the intensity of the new peak increases much more rapidly, signifying a sharp increase in reaction rate, which continues until the end of the experiment. Correspondingly, the intensity of the peaks (between 75 and 86 ppm) due to the  $\text{CaAl}_2\text{O}_4$  starting material decreases relatively slowly during the first 16 h of the reaction, followed by a much more rapid decrease throughout the remainder of the experiment.

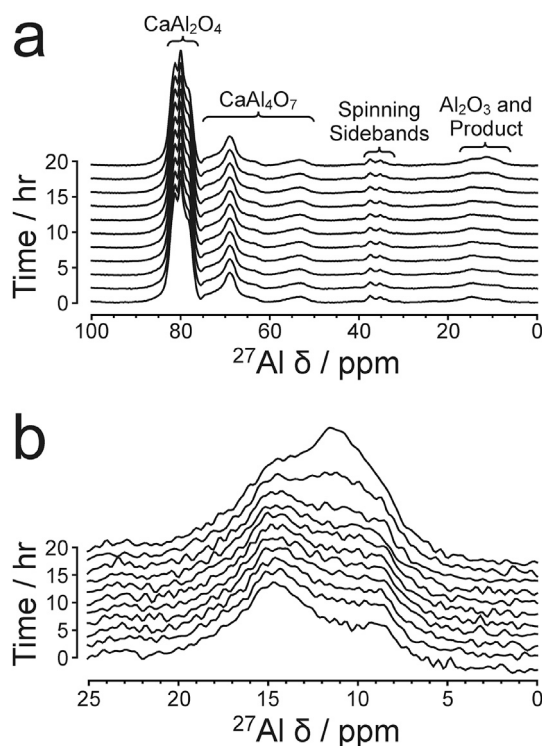


**Fig. 2.** Direct-excitation  $^{27}\text{Al}$  NMR spectra recorded as a function of time during the reaction of CAC with water at 20 °C: (a) the full spectral region from 0 ppm to 100 ppm and (b) expanded spectra showing the region from 0 ppm to 25 ppm.

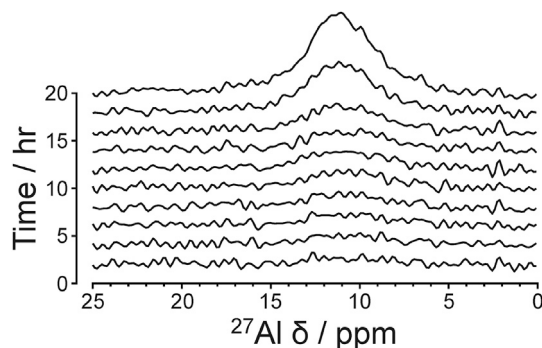


**Fig. 3.** Direct-excitation  $^{27}\text{Al}$  NMR spectra recorded as a function of time during the reaction of CAC with water at 20 °C, following subtraction of the second spectrum recorded. The expanded region from 0 ppm to 25 ppm is shown (as in Fig. 2b).

Our observation that the reaction proceeds in a number of distinct kinetic regimes is consistent with the initial formation of metastable hydrate phases  $\text{CaAl}_2\text{O}_4 \cdot 10\text{H}_2\text{O}$  and/or  $\text{Ca}_2\text{Al}_2\text{O}_5 \cdot 8\text{H}_2\text{O}$  (see Introduction) in the early stages (up to ca. 5 hr) of the hydration of  $\text{CaAl}_2\text{O}_4$ , followed by a period of virtual stagnation (between 5 and 16 h) in which very little further formation of hydration products is observed. Significantly, our isothermal calorimetry data for the reaction at 20 °C (Fig. 5) also show evidence for a slow period (representing the first ca. 18 hr in this experiment) followed by a period with much more rapid reaction.

Following the slow period of the reaction (up to ca. 16 hr in our *in-situ*  $^{27}\text{Al}$  NMR study), the metastable hydrate phases  $\text{CaAl}_2\text{O}_4 \cdot 10\text{H}_2\text{O}$  and  $\text{Ca}_2\text{Al}_2\text{O}_5 \cdot 8\text{H}_2\text{O}$  then convert rapidly to the stable products  $\text{Ca}_3\text{Al}_2\text{O}_6 \cdot 6\text{H}_2\text{O}$  and  $\text{Al}(\text{OH})_3 \cdot x\text{H}_2\text{O}$  [37]. We note that the  $\text{Al}(\text{OH})_3 \cdot x\text{H}_2\text{O}$  produced in this reaction (Equation (3)) is almost always structurally disordered [22] and it is therefore expected to give a significantly broader signal in the  $^{27}\text{Al}$  NMR spectrum than the signals for the

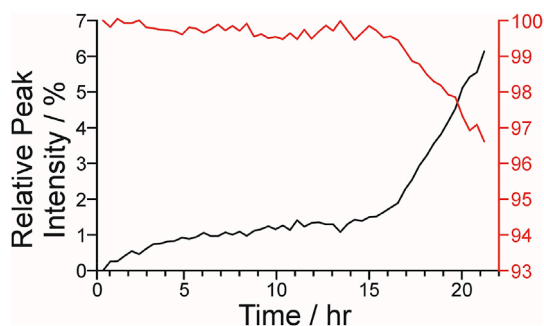


**Fig. 4.** Time-dependence of the intensity of the peaks between 5 and 16 ppm (black; representing the product) and between 75 and 86 ppm (red; representing the reactant) in the direct-excitation  $^{27}\text{Al}$  NMR spectra recorded during reaction of CAC with water at 20 °C. Peak intensities were determined from the spectra after subtracting the second spectrum recorded and are expressed relative to the intensity of the peaks between 75 and 86 ppm for the starting material in the second spectrum.

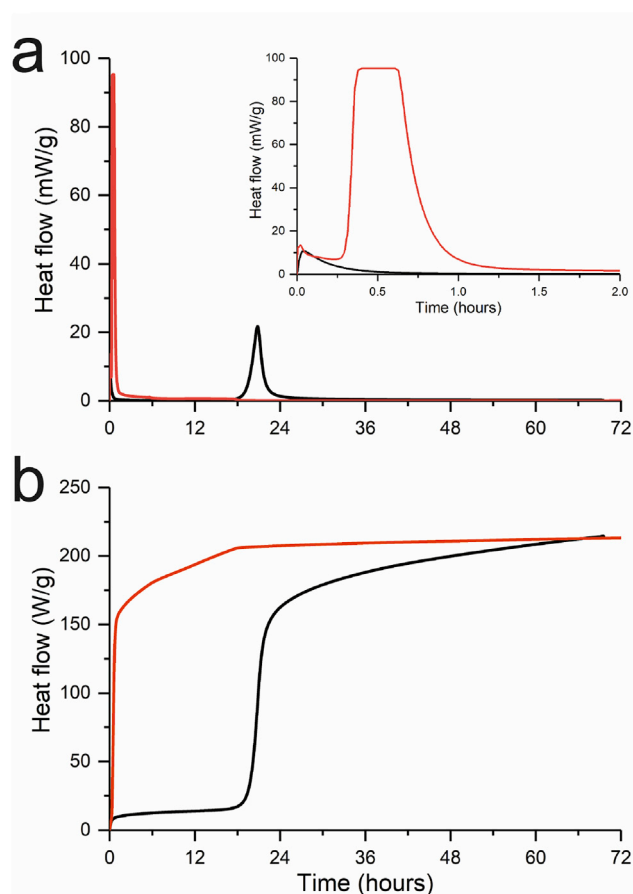


**Fig. 5.** Isothermal calorimetry data showing (a) heat flow and (b) cumulative heat flow as a function of time during the reaction of CAC with water at 20 °C (black) and 60 °C (red).

crystalline products of the hydration reaction. For this reason, the new peak that arises at ca. 11 ppm in the hydration reaction is not expected to contain any significant contribution from  $\text{Al}(\text{OH})_3 \cdot x\text{H}_2\text{O}$ .

Conversion of the initially formed metastable hydrates  $\text{CaAl}_2\text{O}_4 \cdot 10\text{H}_2\text{O}$  and  $\text{Ca}_2\text{Al}_2\text{O}_5 \cdot 8\text{H}_2\text{O}$  to the stable hydrates  $\text{Ca}_3\text{Al}_2\text{O}_6 \cdot 6\text{H}_2\text{O}$  and  $\text{Al}(\text{OH})_3 \cdot x\text{H}_2\text{O}$  in the rapid phase of the reaction (after ca. 16 hr) is associated with release of water [22,38], as shown in Equations (2) and (3). The water released is available to participate in further hydration of the unreacted  $\text{CaAl}_2\text{O}_4$  particles in parallel with

rapid formation of  $\text{Ca}_3\text{Al}_2\text{O}_6 \cdot 6\text{H}_2\text{O}$  and  $\text{Al}(\text{OH})_3 \cdot x\text{H}_2\text{O}$ . This mechanism is consistent with the rapid increase in intensity of the peaks for octahedral  $^{27}\text{Al}$  sites after ca. 16 hr in the direct-excitation  $^{27}\text{Al}$  NMR spectra and with an exothermic process (at ca. 18 hr) in the isothermal calorimetry data (Fig. 5).

For the reaction at 20 °C, MQMAS  $^{27}\text{Al}$  NMR spectra recorded at the beginning of the reaction and after 21 h are shown in Fig. 6. The first spectrum contains two peaks: a broad, high-intensity peak at ca. 80 ppm in the direct (1Q) dimension and at ca. 83 ppm in the indirect (3Q) dimension, which is attributed to tetrahedral  $^{27}\text{Al}$  sites in  $\text{CaAl}_2\text{O}_4$ , and a peak at ca. 68 ppm in the direct (1Q) dimension and at ca. 78 ppm in the indirect (3Q) dimension, which is attributed to tetrahedral  $^{27}\text{Al}$  sites in  $\text{CaAl}_4\text{O}_7$ . After 21 h, a third peak is present, which matches the new peak observed in the direct-excitation  $^{27}\text{Al}$  NMR spectra and is attributed to octahedrally coordinated  $^{27}\text{Al}$  sites in the hydration products.

### 3.3. *In-situ* $^{27}\text{Al}$ NMR study of the hydration reaction at 60 °C

For the reaction at 60 °C, our *in-situ*  $^{27}\text{Al}$  NMR experiment on a mixture of anhydrous CAC and water was run for a total of 22 h. The direct-excitation  $^{27}\text{Al}$  NMR spectra recorded as a function of time after mixing are shown in Fig. 7 (only every fifth recorded spectrum is displayed, with 116 min between the spectra shown). Again, a new peak appears at ca. 11 ppm, superimposed on the peak due to the  $\text{Al}_2\text{O}_3$  impurity phase, and the intensity of this peak grows rapidly. Integration of the new peak (after subtracting the first spectrum from all subsequent spectra) as a function of time gives insights into the kinetics of the hydration reaction (see Fig. 8, in which peak intensity is scaled relative to the intensity of the peaks for the  $\text{CaAl}_2\text{O}_4$  starting material in the first spectrum). In Fig. 8, the decrease in the intensity of the peaks due to  $\text{CaAl}_2\text{O}_4$  (in the region between 75 and 86 ppm) is also shown. The new peak at ca. 11 ppm grows rapidly at the start of the reaction (within the first hour of our experiment) but then slows down to a rate that remains essentially constant for the remainder of the experiment. This behaviour

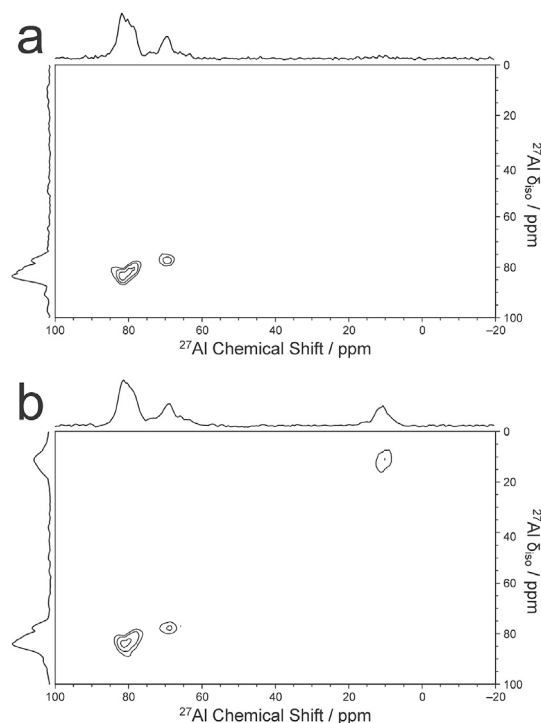


**Fig. 6.** *In-situ* MQMAS  $^{27}\text{Al}$  NMR spectra (acquisition time, 22 min) recorded during the reaction between CAC and water at 20 °C: (a) the first spectrum recorded and (b) the final spectrum recorded (after 21 h). The indirect dimension was scaled according to the Bruker convention.



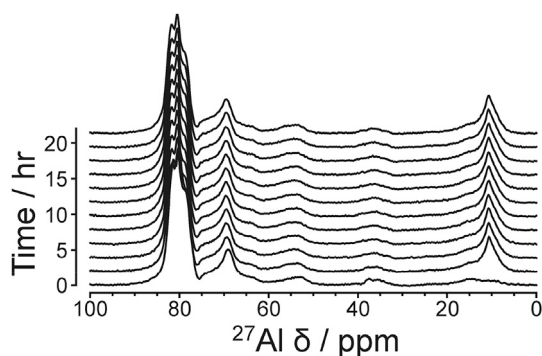


Fig. 7. Direct-excitation  $^{27}\text{Al}$  NMR spectra recorded as a function of time during the reaction of CAC with water at  $60^\circ\text{C}$ .

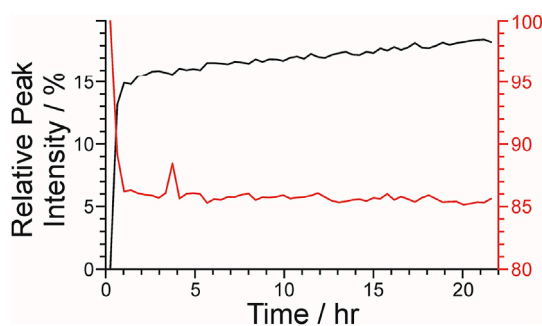


Fig. 8. Time-dependence of the intensity of the peaks between 5 and 16 ppm (black; representing the product) and between 75 and 86 ppm (red; representing the reactant) in the direct-excitation  $^{27}\text{Al}$  NMR spectra recorded during reaction of CAC with water at  $60^\circ\text{C}$ . The peak intensities were determined from the spectra after subtracting the first spectrum recorded and are expressed relative to the intensity of the peaks between 75 and 86 ppm due to the starting material in the first spectrum.

is mirrored by a rapid decrease in the intensity of the peaks due to the  $\text{CaAl}_2\text{O}_4$  starting material within the early period of the reaction, followed by a much slower decrease for the remainder of the experiment.

The first  $^{27}\text{Al}$  MQMAS NMR spectrum acquired at  $60^\circ\text{C}$  contains only peaks due to  $\text{CaAl}_2\text{O}_4$  and  $\text{CaAl}_4\text{O}_7$ . All subsequent MQMAS spectra indicate that these two phases are present, together with a signal corresponding to the new peak observed in the direct-excitation  $^{27}\text{Al}$  NMR spectra. Fig. 9 shows the final MQMAS spectrum recorded during the experiment (after 21 h).

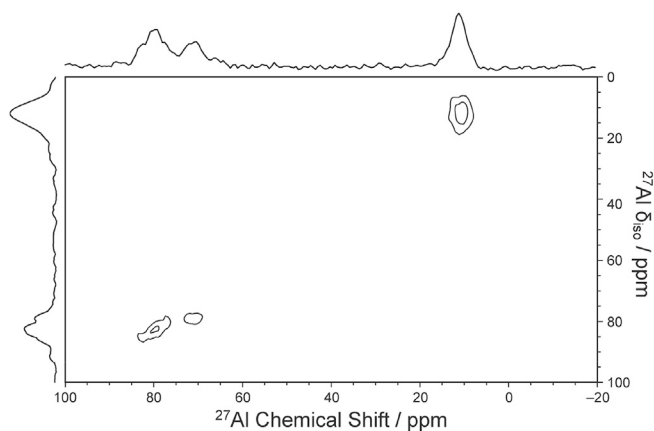


Fig. 9. *In-situ* MQMAS  $^{27}\text{Al}$  NMR spectrum (acquisition time, 22 min) recorded at the end (21 h) of the reaction between CAC and water at  $60^\circ\text{C}$ . The indirect dimension was scaled according to the Bruker convention.

Comparison of Figs. 4 and 8 suggests that there are significant differences in the mechanism of the hydration reaction at  $20^\circ\text{C}$  and  $60^\circ\text{C}$ . At the higher temperature ( $60^\circ\text{C}$ ), the stable hydrate products  $\text{Ca}_3\text{Al}_2\text{O}_6\cdot 6\text{H}_2\text{O}$  and  $\text{Al}(\text{OH})_3\cdot x\text{H}_2\text{O}$  are formed rapidly in the early stages of the reaction, in good agreement with isothermal calorimetry data (Fig. 5). It is possible that the metastable hydrate phases  $\text{CaAl}_2\text{O}_4\cdot 10\text{H}_2\text{O}$  and  $\text{Ca}_2\text{Al}_2\text{O}_5\cdot 8\text{H}_2\text{O}$  are formed as intermediates at  $60^\circ\text{C}$ , but in this scenario, it is clear that the conversion of these phases to the stable hydrate phases is sufficiently rapid that they are not observed within the time-resolution of our *in-situ* solid-state NMR study (i.e., within 23.3 min).

#### 3.4. Comparison of the hydration reactions at $20^\circ\text{C}$ and $60^\circ\text{C}$

At both  $20^\circ\text{C}$  and  $60^\circ\text{C}$ , our direct-excitation  $^{27}\text{Al}$  NMR spectra for the hydrated reaction mixture do not contain any measurable contribution from aluminium in the liquid phase at any stage of the reaction, recognizing that solution-state  $^{27}\text{Al}$  species would give much narrower peaks than those observed. Fig. 10 shows an overlay of the final  $^{27}\text{Al}$  NMR spectra recorded at  $20^\circ\text{C}$  and  $60^\circ\text{C}$ , representing the products present at the end of our experiment at each temperature. Although the peaks for the products at  $20^\circ\text{C}$  is somewhat broader and has an observed maximum at slightly higher chemical shift. The  $^{27}\text{Al}$  chemical shift observed in each case is fully consistent with  $^{27}\text{Al}$  species in sites with approximately octahedral coordination [39]. The fact that the peak due to the products at  $20^\circ\text{C}$  is broader than at  $60^\circ\text{C}$  is consistent with our assertion that the sample at  $20^\circ\text{C}$  contains both metastable hydrate phases  $\text{CaAl}_2\text{O}_4\cdot 10\text{H}_2\text{O}$  and  $\text{Ca}_2\text{Al}_2\text{O}_5\cdot 8\text{H}_2\text{O}$  and the stable hydrate phase  $\text{Ca}_3\text{Al}_2\text{O}_6\cdot 6\text{H}_2\text{O}$  at the time at which the experiment was stopped, representing a distribution of local structural environments for the  $^{27}\text{Al}$  sites. It is clear from Fig. 4 that the reaction to produce the stable hydrate products was still continuing at the end of the experiment at  $20^\circ\text{C}$ , suggesting that some amounts of the metastable hydrate phases were still present.

The significantly different kinetics of the reactions at  $20^\circ\text{C}$  and  $60^\circ\text{C}$  are evident from Figs. 4 and 8. Although temperature was constant throughout the reaction in each case, the rate of reaction varies significantly in different time periods during the experiment. At  $20^\circ\text{C}$ , just over 6% of the  $\text{CaAl}_2\text{O}_4$  had reacted by the end of the experiment (i.e., 21 h) while, at  $60^\circ\text{C}$ , only about 15% of the  $\text{CaAl}_2\text{O}_4$  had reacted by the end of the experiment (i.e., 22 h). Assuming in both cases that  $\text{Ca}_3\text{Al}_2\text{O}_6\cdot 6\text{H}_2\text{O}$  would be the final product of the reaction, we calculate [40] that the amount of water used in our experiments was more than sufficient to allow the reaction to proceed to completion. Thus, in our experiments at both  $20^\circ\text{C}$  and  $60^\circ\text{C}$ , the reaction did not come close to exhausting the available supply of water. It is likely that the extent of reaction may be limited by the expectation that the hydrate phases are formed as a “coating” on the surfaces of the particles of anhydrous  $\text{CaAl}_2\text{O}_4$ , which hinders the access of water to these particles. This situation does not commonly arise at such low reaction extents during CAC hydration, but it

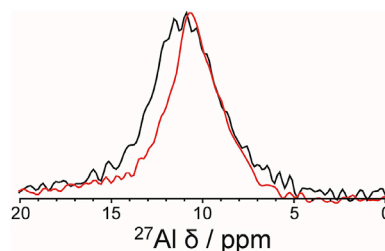


Fig. 10. Overlay of the peaks in the direct-excitation  $^{27}\text{Al}$  NMR spectra from the new phases produced at  $20^\circ\text{C}$  (black) and  $60^\circ\text{C}$  (red). In each case, the last spectrum recorded at the end of the *in-situ*  $^{27}\text{Al}$  NMR study is shown (acquisition time, 1.1 min). The spectra are scaled vertically to give similar peak heights.

is possible that the high-frequency (10 kHz) spinning of the NMR rotor in our experiments may influence the accessibility of water to unreacted particles of anhydrous  $\text{CaAl}_2\text{O}_4$ . Unfortunately, very little information is available about the effects of centrifugation on either the process or products of CAC hydration [41].

#### 4. Concluding remarks

We have demonstrated that the hydration reaction of calcium aluminate cement can be monitored successfully by *in-situ* solid-state  $^{27}\text{Al}$  NMR spectroscopy. We emphasize that the CLASSIC NMR methodology used in this study is sensitive to both the liquid and solid phases present during the reaction, and our results demonstrate that no significant amounts of aluminium species are present in the liquid phase at any stage during the reaction. Within the solid phase, our data provide quantitative information on the change in the relative amounts of  $^{27}\text{Al}$  sites with tetrahedral coordination (the anhydrous reactant phase) and octahedral coordination (the hydrated product phases) as a function of time. At 20 °C, the reaction rate is initially slow but then accelerates substantially after about 16 h while, at 60 °C, the reaction rate is rapid in the early stages and then slows down considerably. The clear difference in kinetic behaviour at these two temperatures underlines the importance of applying time-resolved *in-situ* techniques that are sensitive to monitoring the structural changes that occur in the reacting system as a function of time.

The CLASSIC NMR strategy used in the present study involved alternate recording of direct-excitation and MQMAS  $^{27}\text{Al}$  NMR spectra during the *in-situ* time-resolved study of hydration of CAC, although (as discussed above) it was found that the MQMAS spectra did not reveal any significant additional information for the reaction system under investigation. Nevertheless, the results from the MQMAS spectra are in full support of our interpretation of the direct-excitation  $^{27}\text{Al}$  NMR spectra, and confirm that the observed peaks are definitely from solid phases. Thus, the combined approach of measuring alternating direct-excitation and MQMAS  $^{27}\text{Al}$  NMR spectra was still advantageous compared to simply recording only the direct-excitation  $^{27}\text{Al}$  NMR spectra.

Finally, although our *in-situ* NMR data were recorded under conditions of rapid sample spinning, it is important to note that the timings of the observed events in the reactions at 20 °C and 60 °C are very similar to those observed in our calorimetry experiments (recorded on a static sample). However, we cannot rule out the possibility that centrifugation caused by sample spinning in the NMR measurements may exert some influence on the reaction system under investigation, for example by altering the distribution of water and CAC within the NMR rotor. Further NMR studies of this reaction system carried out as a function of spinning frequency may provide more detailed insights into this issue.

#### Acknowledgements

We are grateful to Cardiff University for financial support and to the U. K. High-Field Solid-State NMR Facility for spectrometer time. The U. K. High-Field Solid-State NMR Facility was funded by EPSRC and BBSRC as well as the University of Warwick, including part funding through Birmingham Science City Advanced Materials Projects 1 and 2 supported by Advantage West Midlands and the European Regional Development Fund. Participation of S.A.B. in this study was funded in part by EPSRC through her Early Career Fellowship (EP/R001642/1). Information on the experimental data that supports the results presented in this paper, together with instructions on how to access this information, can be found in the University of Leeds data catalogue at <https://doi.org/10.5518/558>

#### Appendix A. Supplementary data

Supplementary data to this article can be found online at <https://doi.org/10.1016/j.ssnmr.2019.01.003>.

[org/10.1016/j.ssnmr.2019.01.003](https://doi.org/10.1016/j.ssnmr.2019.01.003).

#### References

- [1] D. Müller, A. Rettel, W. Gessner, G. Scheler, J. Magn. Reson. 57 (1984) 152–156.
- [2] A. Rettel, W. Gessner, D. Müller, G. Scheler, Br. Ceram. Trans. J. 84 (1985) 25–28.
- [3] J. Skibsted, E. Henderson, H.J. Jakobsen, Inorg. Chem. 32 (1993) 1013–1027.
- [4] A.P. Kirchheim, D.C. Dal Molin, P. Fischer, A.-H. Emwas, J.L. Provis, P.J.M. Monteiro, Inorg. Chem. 50 (2011) 1203–1212.
- [5] M.-C. Schlegel, A. Sarfraz, U. Müller, U. Panne, F. Emmerling, Angew. Chem. Int. Ed. 51 (2012) 4993–4996.
- [6] X. Cong, R.J. Kirkpatrick, J. Am. Ceram. Soc. 76 (1993) 409–416.
- [7] A.P. Legrand, H. Sfihi, N. Lequeux, J. Lemaître, J. Biomed. Mater. Res. B Appl. Biomater. 91 (2009) 46–54.
- [8] C.E. Hughes, K.D.M. Harris, J. Phys. Chem. A 112 (2008) 6808–6810.
- [9] C.E. Hughes, K.D.M. Harris, Chem. Commun. 46 (2010) 4982–4984.
- [10] C.E. Hughes, P.A. Williams, T.R. Peskett, K.D.M. Harris, J. Phys. Chem. Lett. 3 (2012) 3176–3181.
- [11] S. Iwama, K. Kuyama, Y. Mori, K. Manoj, R.G. Gonnade, K. Suzuki, C.E. Hughes, P.A. Williams, K.D.M. Harris, S. Veeler, H. Takahashi, H. Tsue, R. Tamura, Chem. Eur. J. 20 (2014) 10343–10350.
- [12] K.D.M. Harris, C.E. Hughes, P.A. Williams, Solid State Nucl. Magn. Reson. 65 (2015) 107–113.
- [13] C.E. Hughes, P.A. Williams, V.L. Keast, V.G. Charalampopoulos, G.R. Edwards-Gau, K.D.M. Harris, Faraday Discuss. 179 (2015) 115–140.
- [14] K.D.M. Harris, C.E. Hughes, P.A. Williams, G.R. Edwards-Gau, Acta Crystallogr. C: Struct. Chem. 73 (2017) 137–148.
- [15] P. Cerreia Vioglio, G. Mollica, M. Juramy, C.E. Hughes, P.A. Williams, F. Ziarelli, S. Viel, P. Thureau, K.D.M. Harris, Angew. Chem. Int. Ed. 57 (2018) 6619–6623.
- [16] A.R. Brough, C.M. Dobson, I.G. Richardson, G.W. Groves, J. Mater. Sci. 29 (1994) 3926–3940.
- [17] E. Pustovgar, R.P. Sangodkar, A.S. Andreev, M. Palacios, B.F. Chmelka, R.J. Flatt, J.-B. d'Espinoze de Lacaille, Nat. Commun. 7 (2016) 10952.
- [18] E. Pustovgar, R.K. Mishra, M. Palacios, J.-B. d'Espinoze de Lacaille, T. Matschei, A.S. Andreev, H. Heinz, R. Verel, R.J. Flatt, Cement Concr. Compos. 100 (2017) 245–262.
- [19] L. Frydman, J.S. Harwood, J. Am. Chem. Soc. 117 (1995) 5367–5368.
- [20] L. Black, P. Purnell, J. Hill, Adv. Appl. Ceram. 109 (2010) 253–259.
- [21] M.C.G. Juenger, F. Winnefeld, J.L. Provis, J.H. Ideker, Cement Concr. Res. 41 (2011) 1232–1243.
- [22] K. Scrivener, in: B.S. Choo (Ed.), Advanced Concrete Technology, Butterworth-Heinemann, Oxford, 2003, pp. 1–31.
- [23] G. Geng, J. Li, Y.-S. Yu, D.A. Shapiro, D.A.L. Kilcoyne, P.J.M. Monteiro, Cryst. Growth Des. 17 (2017) 4246–4253.
- [24] A.N. Christensen, B. Lebeck, D. Sheptyakov, J.C. Hanson, Acta Crystallogr. Sect. B Struct. Sci. 63 (2007) 850–861.
- [25] These limiting temperatures depend to some extent on the availability of water to participate in hydration reactions.
- [26] G.A. Lager, T. Armbruster, J. Faber, Am. Mineral. 72 (1987) 756–765.
- [27] C.E. Hughes, P.A. Williams, K.D.M. Harris, Angew. Chem. Int. Ed. 53 (2014) 8939–8943.
- [28] A. Bielecki, D.P. Burum, J. Magn. Reson. 116 (1995) 215–220.
- [29] A.L. Van Geet, Anal. Chem. 40 (1968) 2227–2229.
- [30] A.L. Van Geet, Anal. Chem. 42 (1970) 679–680.
- [31] A.E. Aliev, K.D.M. Harris, Magn. Reson. Chem. 32 (1994) 366–369.
- [32] S.P. Brown, S.J. Heyes, S. Wimperis, J. Magn. Reson. 119 (1996) 280–284.
- [33] J.-P. Amoureux, C. Fernandez, S. Steuermann, J. Magn. Reson. 123 (1996) 116–118.
- [34] A.P.M. Kentgens, R. Verhagen, Chem. Phys. Lett. 300 (1999) 435–443.
- [35] J. Skibsted, N.C. Nielsen, H. Bildsøe, H.J. Jakobsen, J. Magn. Reson. 95 (1991) 88–117.
- [36] The first spectrum recorded was not used in this analysis as the intensity of the peak due to  $\text{CaAl}_2\text{O}_4$  is significantly higher in the first spectrum, possibly as a result of incomplete spin-lattice relaxation in all subsequent spectra.
- [37] A previous study (ref. 38) of hydration of  $\text{CaAl}_2\text{O}_4$  at 20 °C reported that conversion commenced ca. 48 hr after initial mixing and thereafter continued beyond 28 days.
- [38] H. Fryda, K.L. Scrivener, G. Chanvillard, C. Feron, in: Calcium Aluminate Cements 2001, Institute of Materials, U. K., 2001, pp. 227–246.
- [39] The absence of any significant quadrupolar broadening is also consistent with this assignment, as the quadrupolar interaction (which is zero for a  $^{27}\text{Al}$  site with perfect octahedral symmetry) is expected to be small for  $^{27}\text{Al}$  sites with approximately octahedral local symmetry.
- [40] For the reaction in Equation (4), we calculate that a mass ratio (water to  $\text{CaAl}_2\text{O}_4$ ) of 0.46 is required to allow the reaction to reach completion, corresponding to 100% conversion from  $\text{CaAl}_2\text{O}_4$  to  $\text{Ca}_3\text{Al}_2\text{O}_6 \cdot 6\text{H}_2\text{O}$ . As the mass ratio of the paste used at both temperatures in our experiments was 0.64, it is clear that the ability of the reaction to reach completion is not limited by the total amount of water available in the reaction system.
- [41] We note that, when the rotor inserts were sectioned for visual observation at the conclusion of our experiments, segregation of water from the paste was not observed.
- [42] Note that this spectrum was the first spectrum recorded in our *in-situ*  $^{27}\text{Al}$  NMR study at 20 °C.
- [43] C.E. Hughes, K.D.M. Harris, Solid State Nucl. Magn. Reson. 80 (2016) 7–13.